MRDC41097.3TR

RESEARCH ON FERROELECTRIC MATERIALS FOR MILLIMETER WAVE APPLICATION

Semi-Annual Technical Report No. 1
For Period 08/05/81 through 02/28/82

May 1982

ARPA Order No.	4240
Program Code:	2306/B2
Name of Contractor:	Rockwell International Corporation
Effective Date of Contract:	August 5, 1981
Contract Expiration Date:	August 4, 1982
Amount of Contract Dollars:	$379,182
Contract Number:	F49620-81-C-0090
Principal Investigators:	Dr. R.R. Neurgaonkar (805) 498-4545, Ext. 109 Dr. L.E. Cross Pennsylvania State University (814) 865-1181 Dr. W.F. Hall (805) 498-4545 Ext. 189 Dr. W.W. Ho (805) 498-4545 Ext. 194

Sponsored by

Advanced Research Projects Agency (DoD)
APRA Order No. 4240
Monitored by AFOSR Under Contract No. F49620-81-C-0090

UNCLASSIFIED

SECURITY CLASSIFICATION OF THIS PAGE (When Data Entered)

REPORT DOCUMENTATION PAGE	READ INSTRUCTIONS BEFORE COMPLETING FORM
1. REPORT NUMBER AFOSR-TR- 82-0509 / 2. GOVT ACCESSION NO. AD-A115 868	3. RECIPIENT'S CATALOG NUMBER
4. TITLE (and Subtitle) RESEARCH ON FERROELECTRIC MATERIALS FOR MILLIMETER WAVE APPLICATION	5. TYPE OF REPORT & PERIOD COVERED Semi-Annual Technical Report 08/05/81 through 02/28/82
	6. PERFORMING ORG. REPORT NUMBER MRDC41097,3TR
7. AUTHOR(s) R.R. Neurgaonkar	8. CONTRACT OR GRANT NUMBER(s) F49620-81-C-0090
9. PERFORMING ORGANIZATION NAME AND ADDRESS Rockwell International Microelectronics Research and Development Ctr. 1049 Camino Dos Rios, Thousand Oaks, CA 91360	10. PROGRAM ELEMENT, PROJECT, TASK AREA & WORK UNIT NUMBERS [redacted] 61102F 2306/B2
11. CONTROLLING OFFICE NAME AND ADDRESS Air Force Office of Scientific Research Bolling Air Force Base Washington, D.C. 20332	12. REPORT DATE May 1982
	13. NUMBER OF PAGES 36
14. MONITORING AGENCY NAME & ADDRESS(if different from Controlling Office)	15. SECURITY CLASS. (of this report) UNCLASSIFIED
	15a. DECLASSIFICATION/DOWNGRADING SCHEDULE

16. DISTRIBUTION STATEMENT (of this Report)

Approved for public release; distribution unlimited.

17. DISTRIBUTION STATEMENT (of the abstract entered in Block 20, if different from Report)

18. SUPPLEMENTARY NOTES

19. KEY WORDS (Continue on reverse side if necessary and identify by block number)

20. ABSTRACT (Continue on reverse side if necessary and identify by block number)

A one-year research program has been undertaken to determine whether certain selected ferroelectric materials can be used to obtain effective phase control in millimeter wave radar systems. This investigation is an outgrowth of earlier work at Rockwell which included the first demonstration of microwave phase modulation in strontium barium niobate (SBN) single crystals.[1] The present study combines materials development and millimeter wave characterization to investigate the feasibility of achieving sensitivity of the microwave refractive index to an applied electric field, dn/dE, in excess of

1 cont

DD FORM 1 JAN 73 1473 EDITION OF 1 NOV 65 IS OBSOLETE

UNCLASSIFIED

SECURITY CLASSIFICATION OF THIS PAGE (When Data Entered)

cont

10^{-5} meters/volt, while maintaining absorptive loss in the material below a few dB per millimeter.

Because measurements early in the program revealed high absorptive losses in the available strontium barium niobate crystals, the first six months have been devoted to expanding the materials base. In addition to the development of growth techniques for other tungsten bronze ferroelectrics, measurements of millimeter wave dielectric properties have been carried out on these ferroelectric and other systems obtained from the Penn State Materials Research Laboratory, including an antiferroelectric ceramic lead-lantanum zirconate-titanate (PLZT). These measurements generally show large decreases in polar axis permittivity from their dc values, suggesting an extrinsic origin for the bulk of the dc permittivity. The material factors controlling this phenomenon should be explored, since they will determine to what extent the observed high losses can be reduced over the frequency range of interest.

Accession For	
NTIS GRA&I	X
DTIC TAB	☐
Unannounced	☐
Justification	
By	
Distribution/	
Availability Codes	
Dist	Avail and/or Special
A	

TABLE OF CONTENTS

LIST OF FIGURES

LIST OF TABLES

1.0 SUMMARY

A one-year research program has been undertaken to determine whether certain selected ferroelectric materials can be used to obtain effective phase control in millimeter wave radar systems. This investigation is an outgrowth of earlier work at Rockwell which included the first demonstration of microwave phase modulation in strontium barium niobate (SBN) single crystals.[1] The present study combines materials development and millimeter wave characterization to investigate the feasibility of achieving sensitivity of the microwave refractive index to an applied electric field, dn/dE, in excess of 10^{-5} meters/volt, while maintaining absorptive loss in the material below a few dB per millimeter.

Because measurements early in the program revealed high absorptive losses in the available strontium barium niobate crystals, the first six months have been devoted to expanding the materials base. In addition to the development of growth techniques for other tungsten bronze ferroelectrics, measurements of millimeter wave dielectric properties have been carried out on these ferroelectric and other systems obtained from the Penn State Materials Research Laboratory, including an antiferroelectric ceramic lead-lantanum zirconate-titanate (PLZT). These measurements generally show large decreases in polar axis permittivity from their dc values, suggesting an extrinsic origin for the bulk of the dc permittivity. The material factors controlling this phenomenon should be explored, since they will determine to what extent the observed high losses can be reduced over the frequency range of interest.

Technical Problem

On the basis of current models for ferroelectric materials, one predicts that certain ferroelectrics having a high dc permittivity $\varepsilon(o)$ should also show high sensitivity of their microwave refractive index $n = \sqrt{\varepsilon(\omega)}$ to an applied electric field for microwave frequencies up to several hundred GHz. A low absorptive loss is also predicted over the same range of frequencies.

However, the millimeter wave dielectric properties of these materials are largely unknown, and growth of the most promising ferroelectrics in single crystal form is generally difficult.

The present program was conceived on the basis of successful growth at Rockwell of one such ferroelectric, $Sr_{0.61}Ba_{0.39}Nb_2O_6$, and measurement in this material of a substantial electric field sensitivity, dn/dE, of 10^{-6} meters/volt at 58 GHz.[1] With about an order of magnitude larger sensitivity, one can design microwave components operating at practical control voltages (under 200 volts) for phase shifting, modulation, and switching. One attractive concept is a planar dielectric lens for electronically steering a millimeter wave radar beam, which could be used in high-speed seeker applications.

The technical objective of the current study is to explore the range of dielectric properties (primarily dn/dE and dielectric loss) achievable within the SBN family. Other promising ferroelectrics are to be examined depending on availability.

General Methodology

There is an on-going program in development of growth techniques for tungsten-bronze materials at Rockwell which provides the principal source for the $Sr_{1-x}Ba_xNb_2O_6$ ferroelectrics to be studied under the present contract. This program has produced the largest and highest quality single crystals reported to date of $Sr_{0.69}Ba_{0.31}Nb_2O_6$, the congruently melting composition.[2] Having these crystals available as seeds greatly facilitates the Czochralski growth of other SBN compositions and certain other tungsten bronzes. Also, through the ferroelectrics program at Penn State University, a wide variety of other materials has been made available for this study. These include ferroelectric and antiferroelectric ceramics as well as single crystals, many of which have been well characterized by piezoelectric and low frequency dielectric measurement techniques.

Accurate high-frequency dielectric measurements on the selected systems are being carried out in waveguide from 30 to 100 GHz.[3] Power reflection

and transmission coefficients are determined on samples cut to fill the guide, and sample dielectric properties are fitted to these observations. The electric field sensitivity of the microwave refractive index, dn/dE, is to be evaluated by a phase bridge technique in the same waveguide geometry.

Technical Results

Millimeter wave measurements at selected temperatures have been carried out to date on the following systems: $Sr_{1-x}Ba_xNb_2O_6$ single crystals ($x = 0.39$ and 0.5) at 30-40 GHz; $Pb_{1-y}La_yZr_{0.8}Ti_{0.2}O_3$ ceramic ($y = 0.08$ and 0.10) at 30-40 GHz and 90-100 GHz; and a $Ba_{1.2}Sr_{0.8}K_{0.75}Na_{0.25}Nb_5O_{15}$ single crystal at 90-100 GHz. Typically, all systems showed unexpectedly high dielectric loss ($\tan \delta > 0.1$) and large decreases in the magnitude of the polar axis permittivity from its low-frequency value. In the single crystal systems, permittivities in the plane perpendicular to the polar axis generally did not show a decrease, but measured losses were still high.

These results contradict the simple soft-mode model for the low frequency dielectric properties, which would predict no substantial decrease in polar axis permittivity below several hundred GHz and correspondingly low loss. The observations suggest that the large dc permittivities in the systems under study are associated with a polarization mechanism which relaxes at GHz frequencies. Domains of submicron dimension, stabilized by extrinsic factors, could explain some features of the data.

Implications for Further Research

Until the source of the observed dielectric behavior is determined, no definite conclusions can be drawn concerning the millimeter wave device potential of these materials. If extrinsic factors control the magnitude and frequency dependence of the observed dielectric properties, it may be possible to modify these properties substantially through changes in growth and preparation; for instance, shifting the region of high loss and low permittivity to much higher frequencies. If the mechanism is intrinsic to these systems,

then other classes of ferroelectrics offer promise, and should be studied to establish the range of properties available at millimeter wave frequencies. Field-induced change of phase (e.g., antiferroelectric to paraelectric) and ferroelectric domain switching are strong candidates for consideration.

2.0 BULK SINGLE CRYSTAL GROWTH

The Czochralski single crystal growth technique has successfully been developed to produce large size single crystals of the ferroelectric composition $Sr_{0.5}Ba_{0.5}Nb_2O_6$. Although both the end members $SrNb_2O_6$ and $BaNb_2O_6$ do not belong to the tungsten-bronze family, the solid solution $Sr_{1-x}Ba_xNb_2O_6$, where $0.25 > x > 0.75$, crystallizes in the tetragonal tungsten bronze structure.[4] Figure 1 shows the limit of solid solubility range for the three different phases, e.g., $SrNb_2O_6$, $BaNb_2O_6$ and $Sr_{1-x}Ba_xNb_2O_6$, and the variation of the ferroelectric phase transition temperature for the tungsten-bronze solid solution. This tungsten-bronze solid solution has been shown to be very useful for several device applications since it exhibits the largest electro-optic[5] and pyroelectric coefficients of any well behaved materials.[6] According to our current work, this solid solution possesses temperature compensated orientations[7] and should also be useful for millimeter wave applications.

Most recent work by Megumi et al,[8] indicates that the composition $Sr_{0.60}Ba_{0.40}Nb_2O_6$ (SBN:60) is the only congruently melting composition of the entire series. Figure 2 shows the composition shifts from melt to crystal for the various compositions in the $SrNb_2O_6$-$BaNb_2O_6$ binary system. The Czochralski growth technique has already been established for the composition $Sr_{0.6}Ba_{0.4}Nb_2O_6$, and crystals as large as one-inch diameter have been developed. This technique can be applied to other compositions within this solid solution. Although the composition $Sr_{0.5}Ba_{0.5}Nb_2O_6$ is not congruently melting, it exhibits interesting ferroelectric and optical properties; it was selected in the present work to compare its high frequency dielectric properties to those of SBN:60 and thereby obtain information on the range of properties available in the SBN system. The bulk single crystal growth of this composition has been reported by several workers and the results of these investigations have been summarized in Table 1.

Initially, the SBN:50 crystals were pulled using SBN:60 crystals as seeds, and this proved successful in obtaining reasonably large seed material

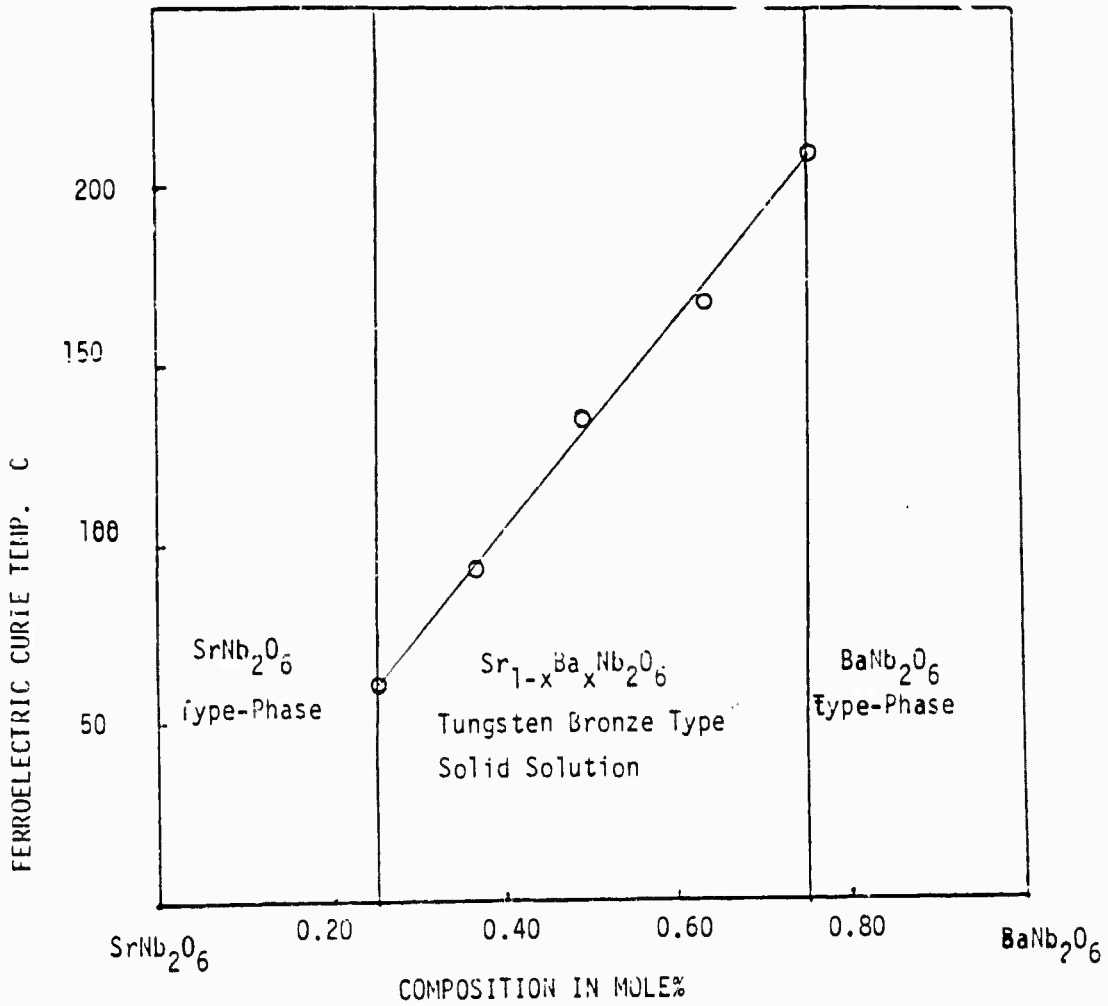

Fig. 1 Phase boundary and Curie temperatures vs composition for $Sr_{1-x}Ba_xNb_2O_6$.

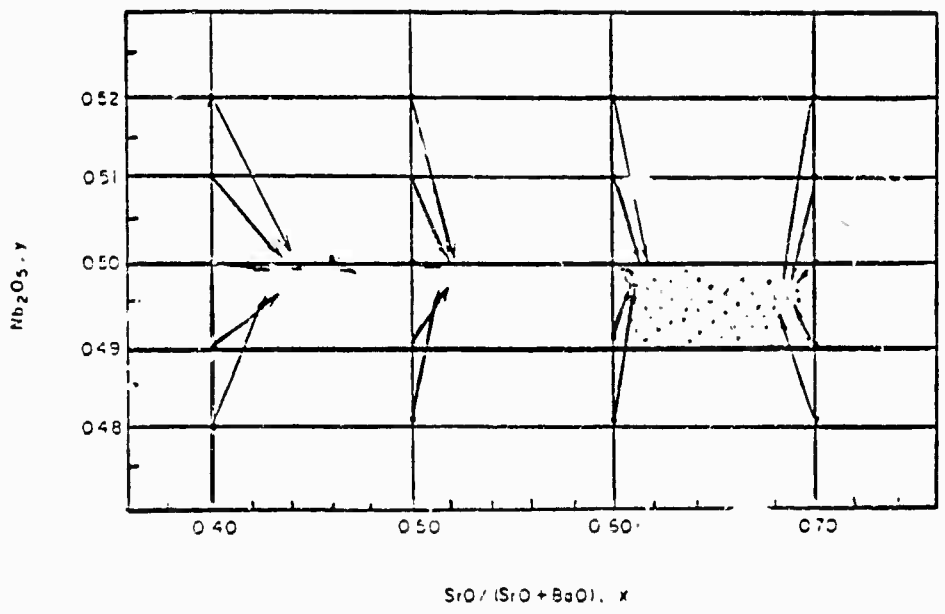

Fig. 2 Composition shift from melts to crystal. Dotted area: area containing congruent melting composition of SBN.

Table 1. Summary of Crystal Growth Conditions for $Sr_{1-x}Ba_xNb_2O_6$ Composition

Composition	Growth Temp °C	Seed Orientation	Diameter of Crystals	Reference
$Sr_{0.5}Ba_{0.5}Nb_2O_6$	1480	(001)	0.5 to 0.8 cm	Kestegian & Bekebrede, 1973
$Sr_{0.5}Ba_{0.5}Nb_2O_6$ (also with R.E.)	1485	(001)	0.3 to 0.5 cm	Liu & Maciolek, 1975
$Sr_{0.5}Ba_{0.5}Nb_2O_6$:Pb	1500	(001)	0.3 to 0.5 cm	Liu & Maciolek, 1975
$Sr_{1-x}Ba_xNb_2O_6$ $0.25 > x > 0.75$	1510	(001)	~1 cm	Ballman & Brown, 1967
$Sr_{0.75}Ba_{0.25}Nb_2O_6$	1485	(001)	-	Sakamoto, Unoki, et al 1973
$Sr_{0.61}Ba_{0.39}Nb_2O_6$	1500	(001)	-	Furuhata, et al, 1976
$Sr_{0.61}Ba_{0.39}Nb_2O_6$	1510	(001)	~2 cm	Neurgaonkar, Kalisher, Lim & Staples, present work
$Sr_{0.5}Ba_{0.5}Nb_2O_6$	1510	(001)	~2 cm	Neorgaonkar et al

F.E. → Rare Earths

for subsequent growth experiments. Optimum growth conditions used are as follows:

1.	The pulling rate	8-10 mm/hr
2.	The rotation rate	20-30 rpm
3.	Growth direction	Along the c-axis
4.	Melting temperature	1510°C

The crystals were also pulled along other orientations such as (100) and (110) and under different experimental conditions. However, it was found difficult to obtain large crystals in other directions. This clearly suggested that the rate of crystallization along the c-axis is much faster than that along any other direction. Figure 3 shows a typical crystal grown along the c-axis. The crystals grown along the c-axis are usually well faceted, which is quite exceptional for the Czochralski grown crystals. X-ray diffraction studies show that the crystal habits are based on 24 faces of four prisms: (110), (120), (100) and (130). These observations are in excellent agreement with results reported by Dundnik et al[9] for the $Sr_{1-x}Ba_xNb_2O_6$ solid solution single crystals. The idealized form of the crystal is shown in Fig. 4. The crystals are pale yellow to yellow as grown depending on the crystal diameter. Since the ferroelectric phase transition temperature for this composition occurs around 120°C, the crystals were cooled with utmost care to room temperature to prevent cracking of the grown crystals.

Optically, the $Sr_{0.5}Ba_{0.5}Nb_2O_6$ single crystals appear to be good quality crystals that are clear and transparent. Crystals showed room temperature tungsten-bronze tetragonal structure and, according to the structural refinements by Jamieson et al[10] for $Sr_{0.75}Ba_{0.25}Nb_2O_6$ crystals, this solid solution belongs to the point group 4 mm. The lattice parameter measurements for the ceramic and single crystal samples of the $Sr_{0.5}Ba_{0.5}Nb_2O_6$ composition gave values of a = 12.488Å and c = 3.956Å, which are in close agreement with the values a = 12.48Å and c = 3.950Å reported by Jamieson et al for the same composition.

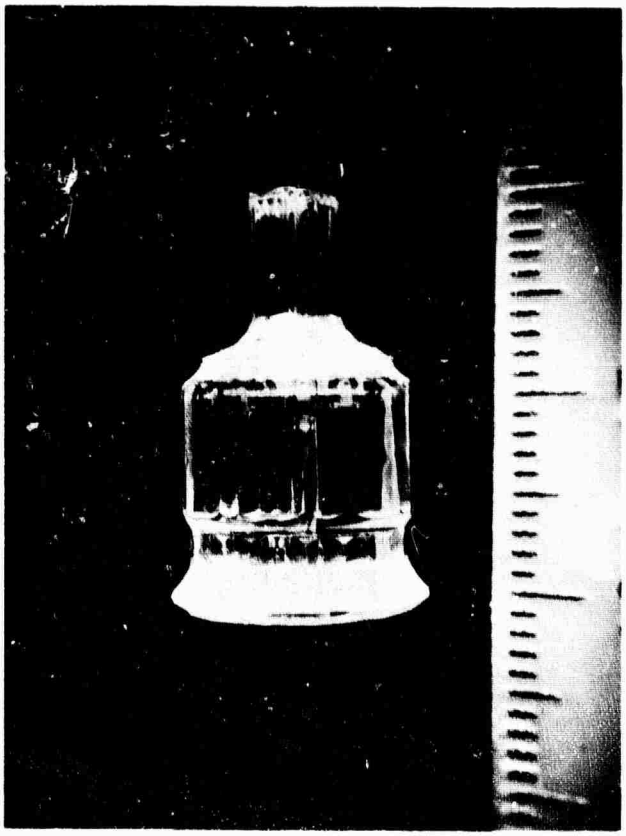

Fig. 3 Shows a typical $Sr_{0.5}Ba_{0.5}Nb_2O_6$ single crystal grown along the c-axis.

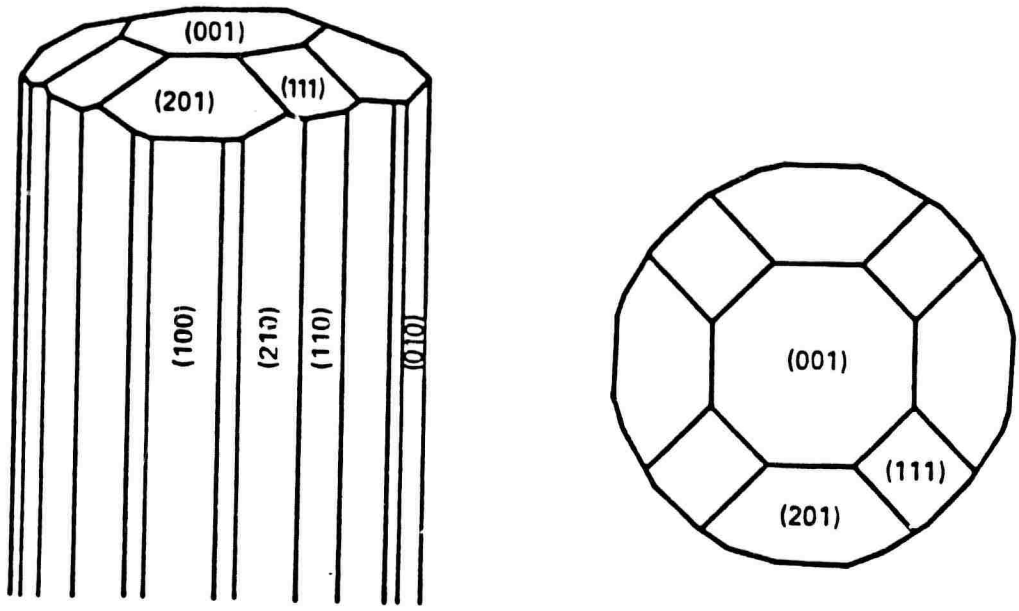

Fig. 4 Shows the idealized form of the SBN single crystal.

3.0 DIELECTRIC CHARACTERIZATION

The initial experimental success in demonstrating a large electric field sensitivity, $dn/dE \sim 10^{-6}$ meters/volt, in the congruently melting SBN composition[1] has provided a natural direction for the current study. Since both the low frequency and optical properties of SBN are known to be strong functions of the strontium to barium ratio, our first priority has been to characterize the range of millimeter wave dielectric properties available in this system. Toward this end, the permittivity and dielectric loss in single crystal samples of the congruently melting composition (SBN:60) were determined from 30 to 40 GHz by reflection and transmission measurements made in waveguide.[3]

These measurements revealed several surprising features: polar axis permittivities much smaller than the low frequency value, with large variation from sample to sample; high loss ($\tan \delta > 0.2$) in all samples; and rapid variation (dispersion) in permittivity with frequency. Such behavior directly contradicts the soft-mode model for the permittivity, which predicts no significant variation from the low frequency properties up to frequencies of several hundred GHz. Also of concern is the high dielectric loss, which represents a substantial barrier to millimeter wave device applications.

With the source of the observed dielectric properties in doubt, it was recognized that a wider experimental base was needed. In particular, a search for factors affecting the dielectric loss has been undertaken. Other tungsten-bronze ferroelectrics, including SBN:50, are currently being studied. Also, an antiferroelectric PLZT ceramic has been characterized up to 100 GHz.

3.1 Dielectric Properties of SBN:60

Figures 5-8 summarize the results of our dielectric measurements on the congruently melting composition $Sr_{0.61}Ba_{0.39}Nb_2O_6$. The polar axis permittivity K'_{33} and the loss tangent K''_{33}/K'_{33} for frequencies between 30 and

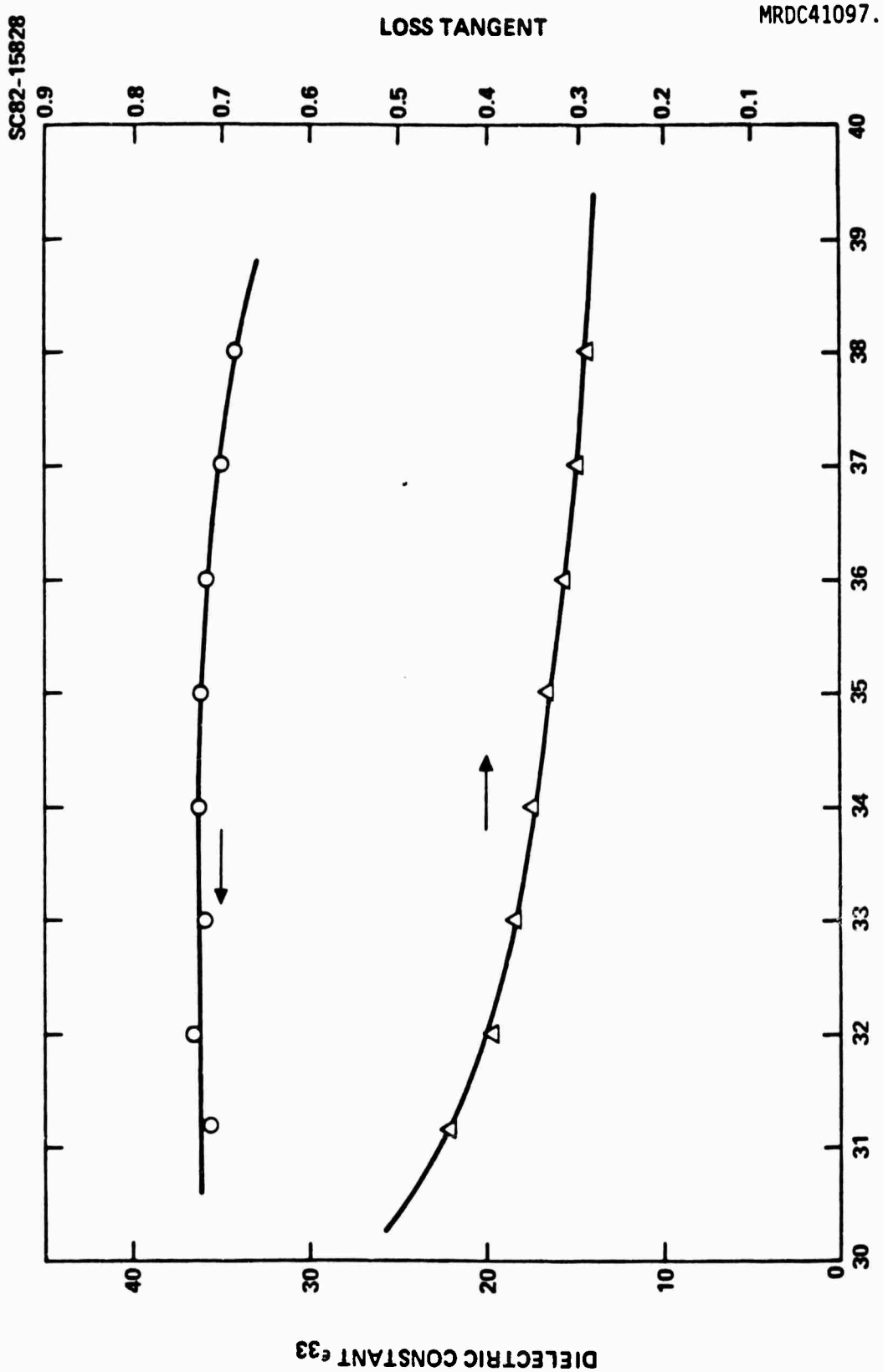

Fig. 5 Measured dielectric constant K'_{33} and loss tangent for an SBN:60 single crystal sample between 30 and 40 GHz.

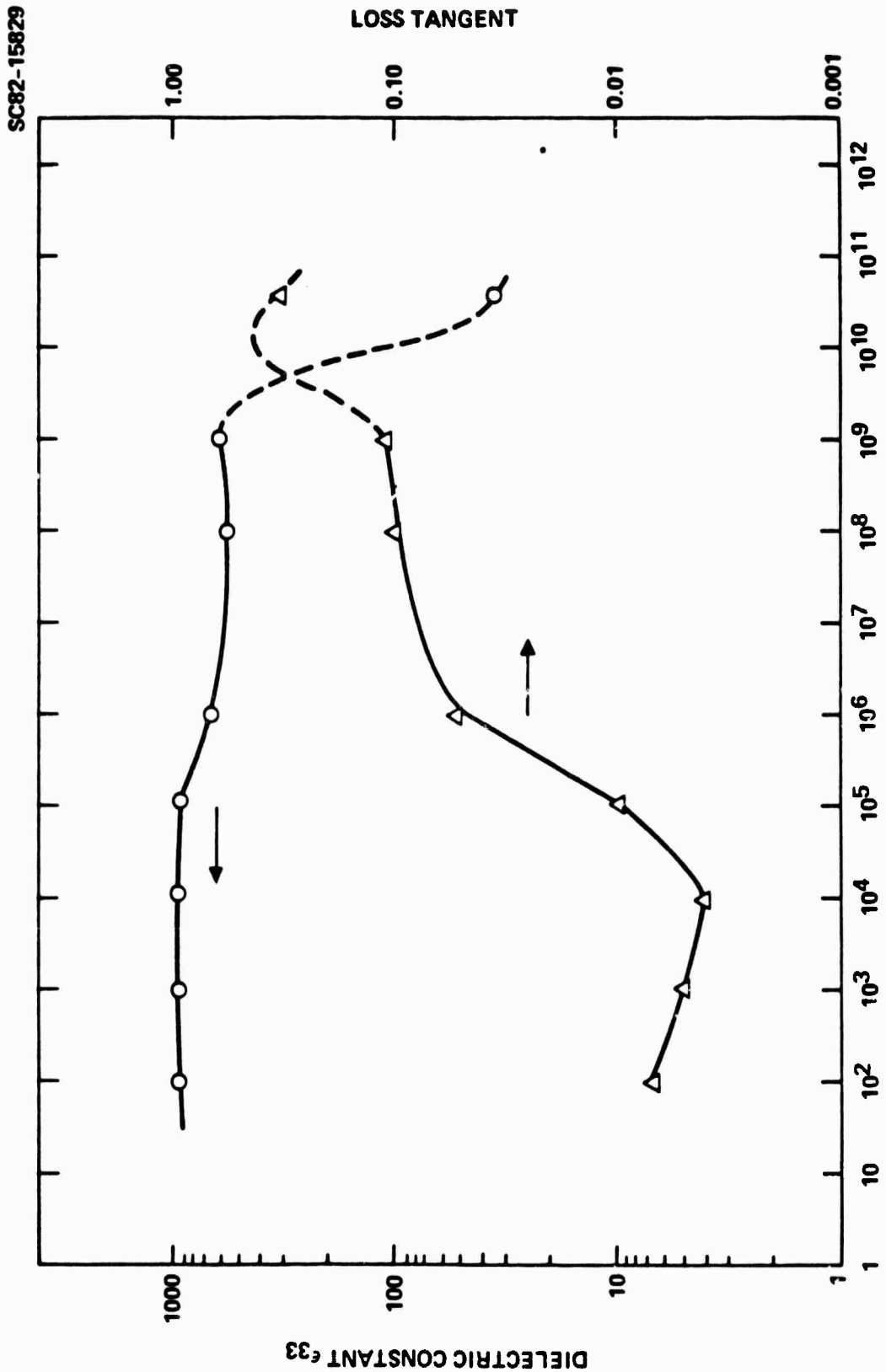

Fig. 6 Measured frequency dependence of dielectric properties along the polar axis for the sample of Fig. 5.

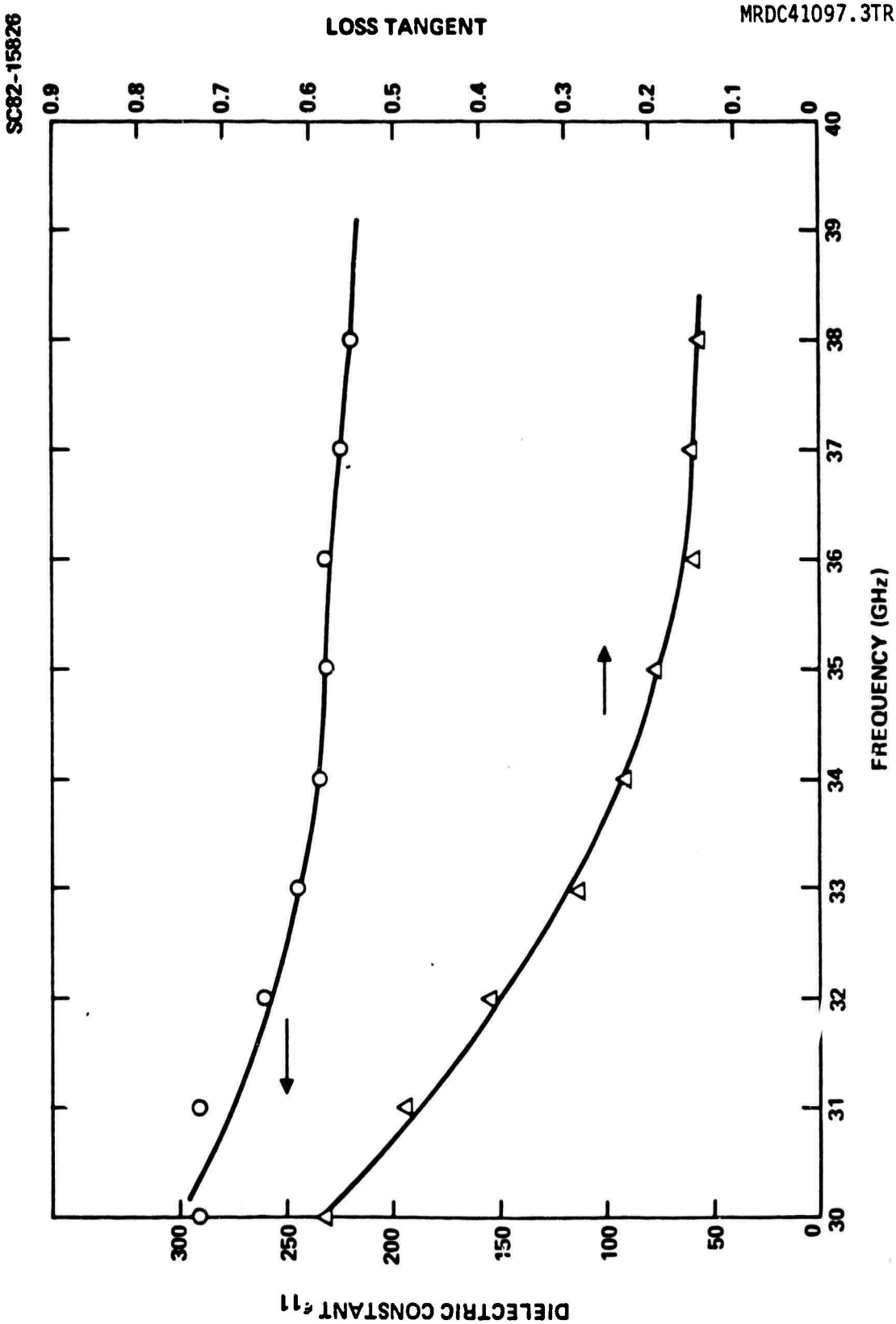

Fig. 7 Measured dielectric constant K_{11} and loss tangent for an SBN:60 single crystal sample between 30 and 40 GHz.

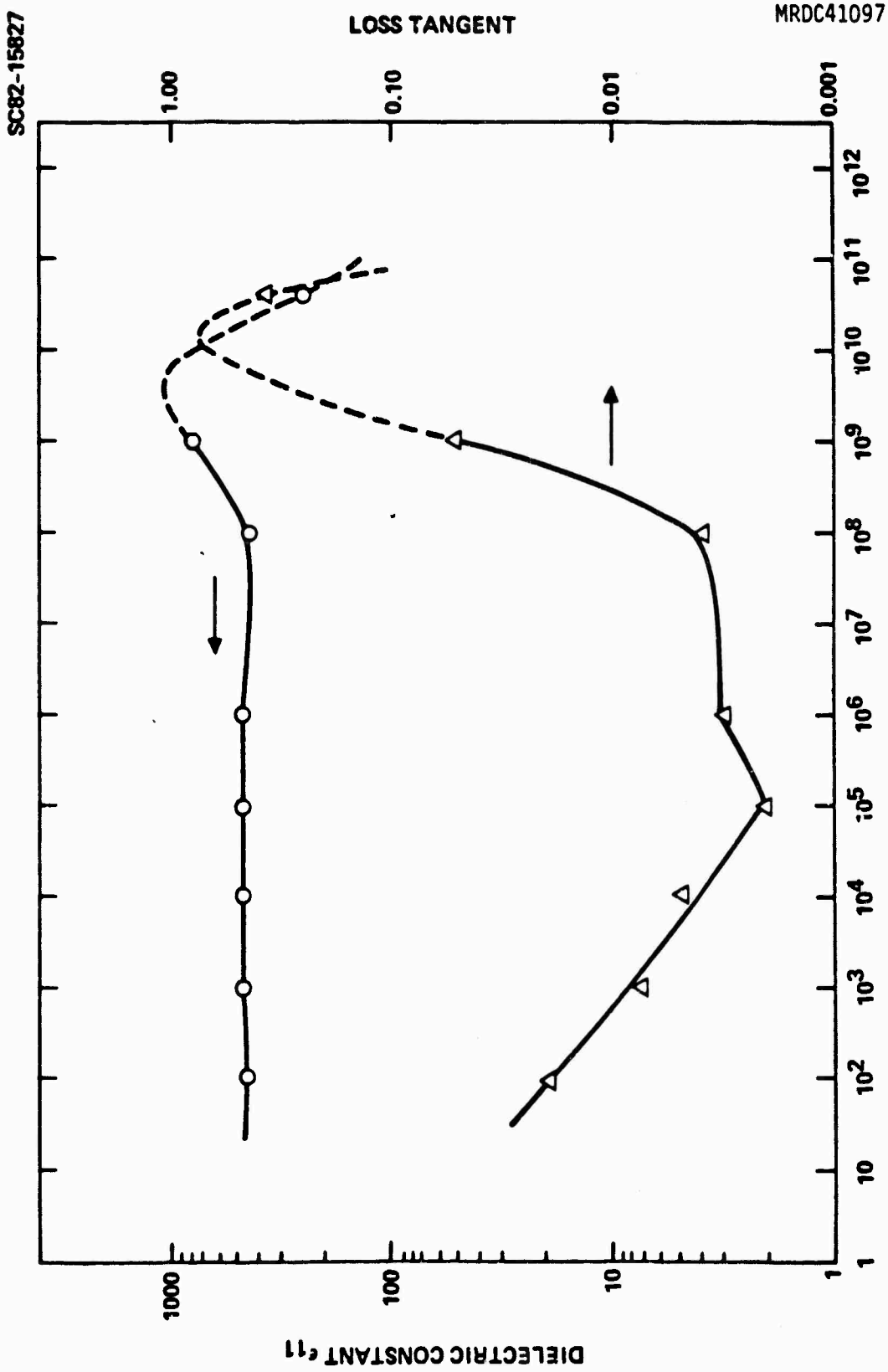

Fig. 8 Measured frequency dependence of dielectric properties perpendicular to the polar axis for the sample of Fig. 7.

40 GHz are shown in Fig. 5 for a carefully poled sample from a recent growth. This sample was selected to show a maximum observed decrease in K'_{33} from its low frequency value of 900; another sample from the same boule showed K'_{33} varying from 100 to 200, while a sample from an earlier growth showed K'_{33} in the range 170 to 300. One observable difference among these samples is the spacing of striations along the growth axis, which is indicative of small variations in composition due to thermal gradients at the solid-liquid interface during growth of the crystals.

The variation of K'_{33} and tan δ_{33} from dc to 40 GHz is illustrated in Fig. 6. The high frequency measurements on this scale show on each curve as a single point and a slope. The dashed sections of the two curves have been sketched to match this behavior to the 1 GHz measurements. All low frequency measurements were carried out at the Penn State Materials Research Laboratory. It is worthy of note that these low-frequency properties showed little variation between the two samples cut from the same boule.

The permittivity perpendicular to the polar axis, K_{11}, is shown for another sample from 30 to 40 GHz in Fig. 7. There is a very rapid decrease in the loss, which suggests we are on the shoulder of a loss peak. Such a peak has been sketched in Fig. 8, where the high frequency measurements are joined with the low frequency data on this sample. The low-frequency data also show a rise in K'_{11} at 1 GHz, which is suggestive of piezoelectric resonance behavior. Domains of submicron size could exhibit such resonances; possibly, point defects or dislocations associated with the growth striations may act to stabilize these domains against poling.

3.2 Measurements on Other Ferroelectrics

A limited number of exploratory measurements have now been carried out on other systems. Results from 30 to 40 GHz for a single crystal sample of SBN:50 grown at this laboratory are shown in Fig. 9 for permittivity perpendicular to the polar axis; it is qualitatively similar to the behavior seen in SBN:60 for the same crystal orientation.

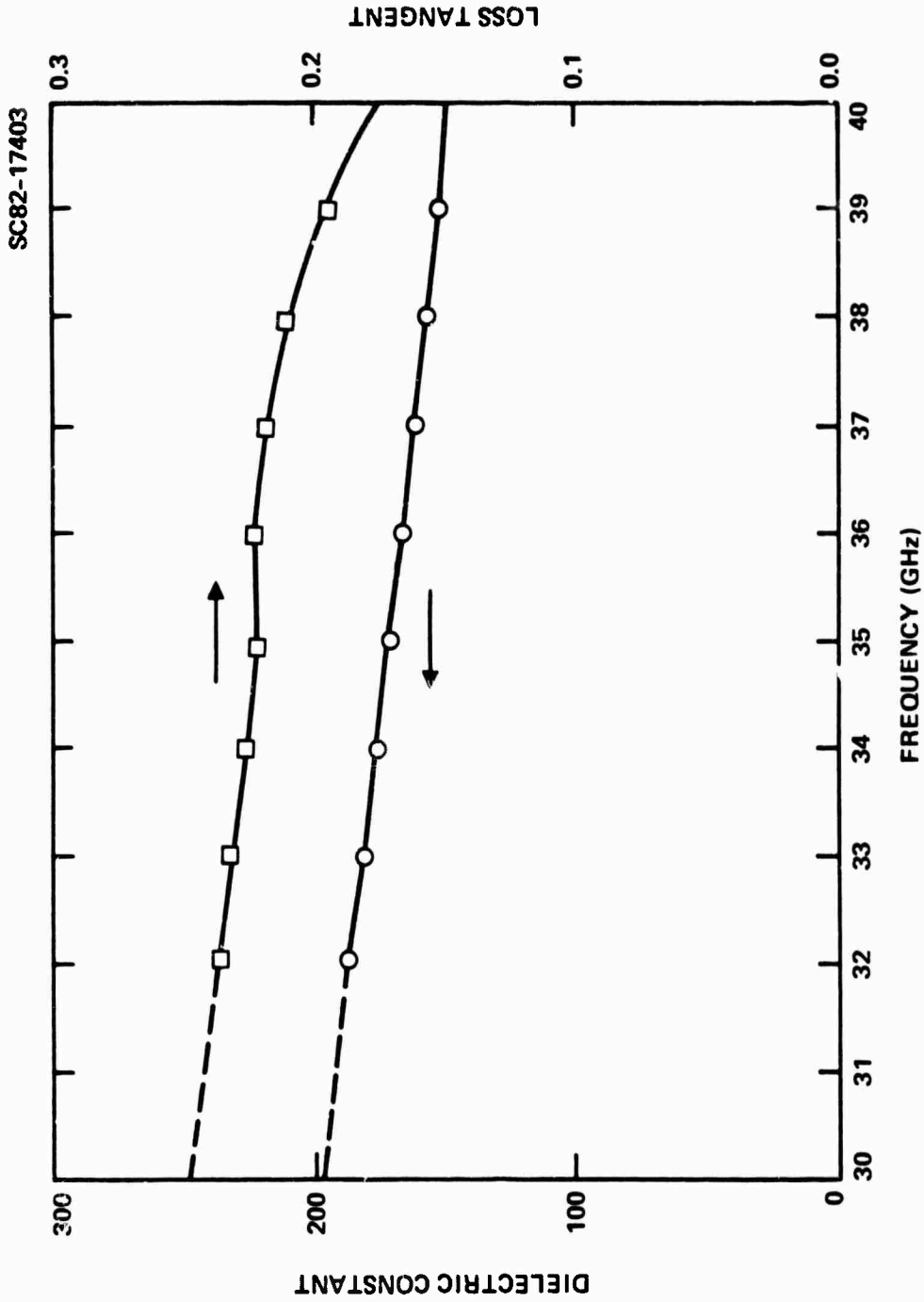

Fig. 9 Dielectric properties of SBN:50 along the a-axis.

A small sample of a "stuffed" tungsten-bronze structure, $Ba_{1.2}Sr_{0.8}K_{0.75}Na_{0.25}Nb_5O_{15}$, was measured from 90 to 100 GHz to see whether filling the vacant cation sites in SBN reduces the loss. These measurements, presented in Fig. 10 show that the perpendicular permittivity (K'_{11}) has not fallen from its low-frequency value, while the associated loss tangent is somewhat lower than those reported above ($\tan \delta_{11} \sim 0.1$). Growth of larger BSKNN crystals is presently being pursued so that measurements in both crystal orientations can be made at 30 to 40 GHz.

A substantial amount of high-frequency dielectric characterization has been carried out on the antiferroelectric ceramic lead-lanthanum zirconate-titanate (PLZT) using samples from Penn State Materials Research Laboratory. The system possesses a large low-frequency dielectric permittivity (~1,000) and is known to switch into a ferroelectric state of much lower permittivity on the application of an electric field of several kilovolts/cm. Since there are no domains in the antiferroelectric phase, loss and dispersion due to domain switching should not contribute to the observed high-frequency dielectric properties of this phase.

Results from 30 to 40 GHz on two samples of the composition $Pb_{0.9}La_{0.1}Zr_{0.8}Ti_{0.2}O_3$ are summarized in Figs. 11-13. The real permittivity (Fig. 11) is quite similar between the two samples, falling from about 400 to 260 over the range of measurements compared to a low frequency value of 1,500. Although not shown, the variation of this permittivity with temperature up to 130°C was found to be small. The loss tangent found for the two samples is shown in Figs. 12 and 13 for three temperatures. While there is a definite similarity between the two, sample #2 shows a generally higher loss. In both cases, losses grow with temperature at the low frequency end of the measurement interval and fall with temperature at the high frequency end, suggesting an underlying loss peak that moves to lower frequency as the temperature is raised.

Room-temperature measurements have also been carried out on these samples from 90 to 100 GHz. Results of these measurements, combined with data

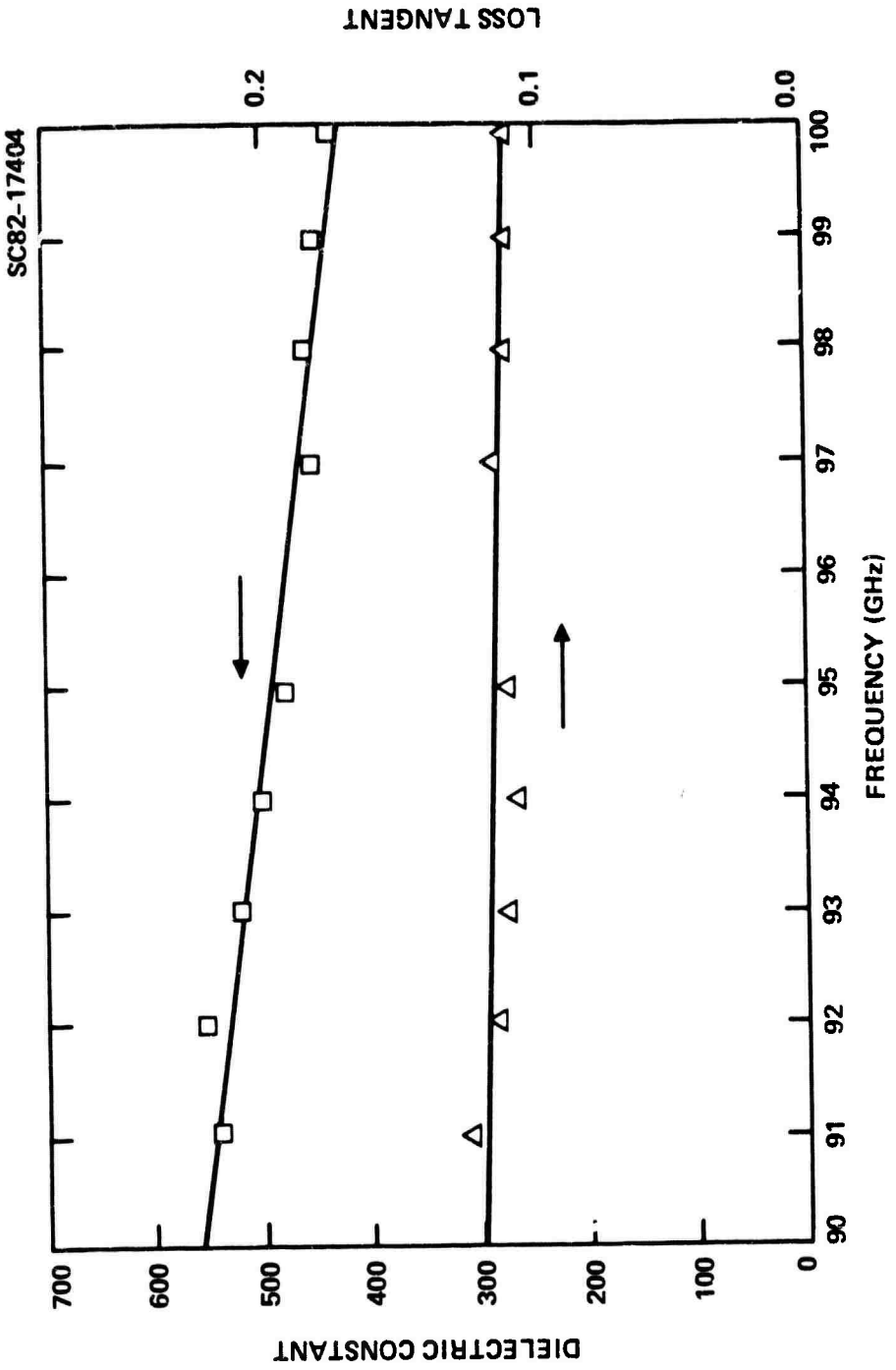

Fig. 10 Dielectric properties of BSKNN along the a-axis.

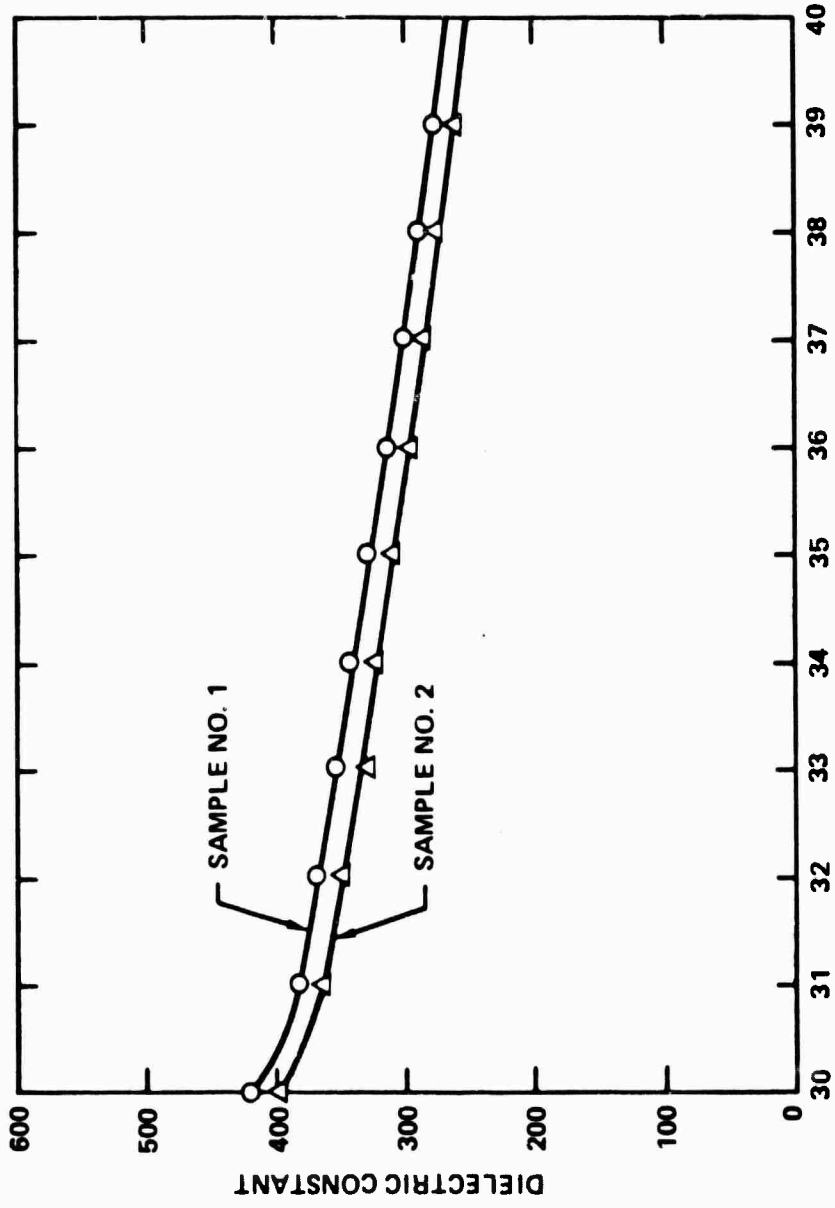

Fig. 11 Measured dielectric constant for ceramic PLZT (La = 10%, Zr/Ti = 80/20).

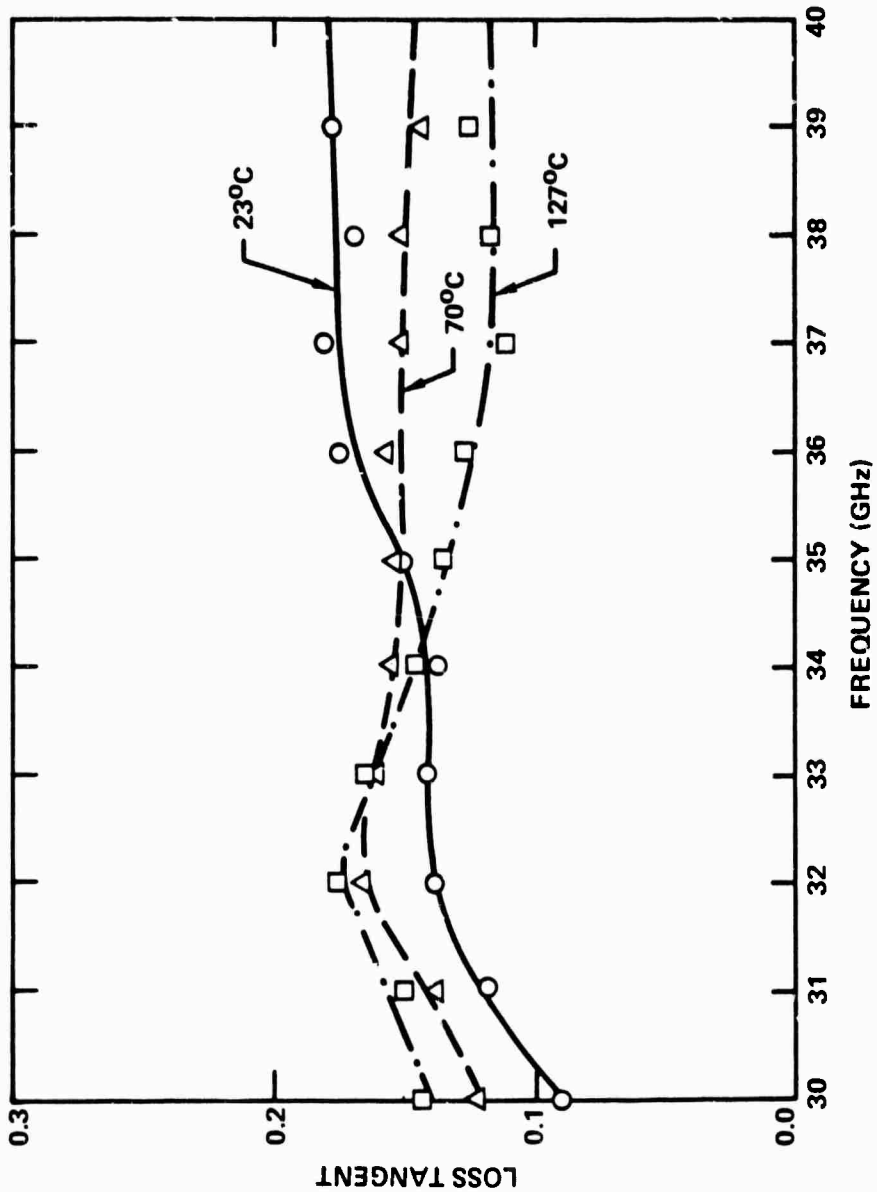

Fig. 12 Loss tangent for ceramic PLZT sample #1 (La = 10%, Zr/Ti = 80/20.

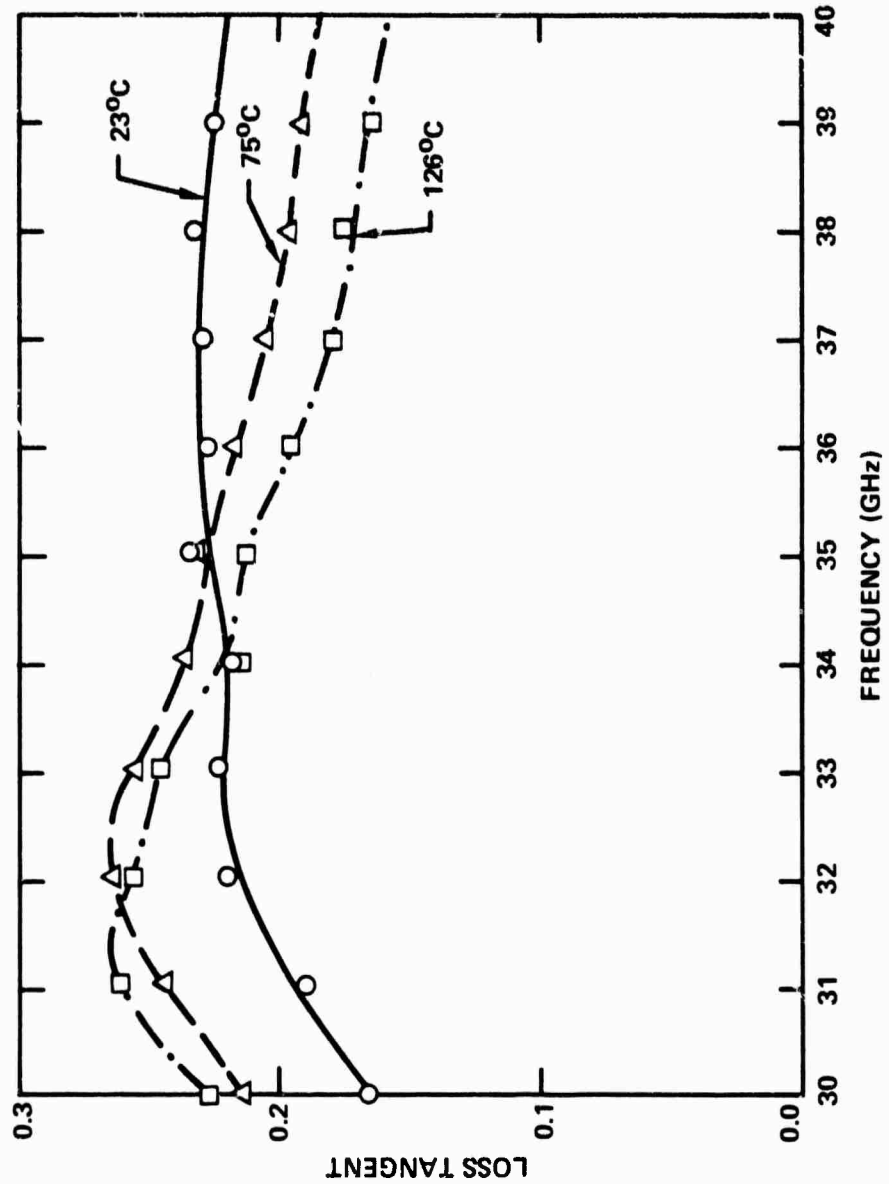

Fig. 13 Loss tangent for ceramic PLZT sample #2 (La = 10%, Zr/Ti = 80/20).

on the low frequency dielectric properties, are given in Fig. 14. One sees that the measured high-frequency loss fits the pattern of slow increase found at lower frequencies. In contrast, the real permittivity is falling rapidly at high frequency, while it is essentially constant below 100 MHz.

The effect of temperature on the dielectric properties at various frequencies is summarized in Fig. 15. The transition to paraelectric form is easily seen in the low frequency data as a broad peak in the permittivity. However, the high frequency data are all essentially temperature independent.

The high-frequency behavior of the complex permittivity in these ceramics is not what one expects for a pure antiferroelectric. However, it is known that an appreciable volume fraction of the PLZT persists in the ferroelectric phase, and the observed dispersion and high loss may well originate in that phase. Experiments in which this volume fraction is varied by control of ceramic composition should help to elucidate the mechanism producing this behavior.

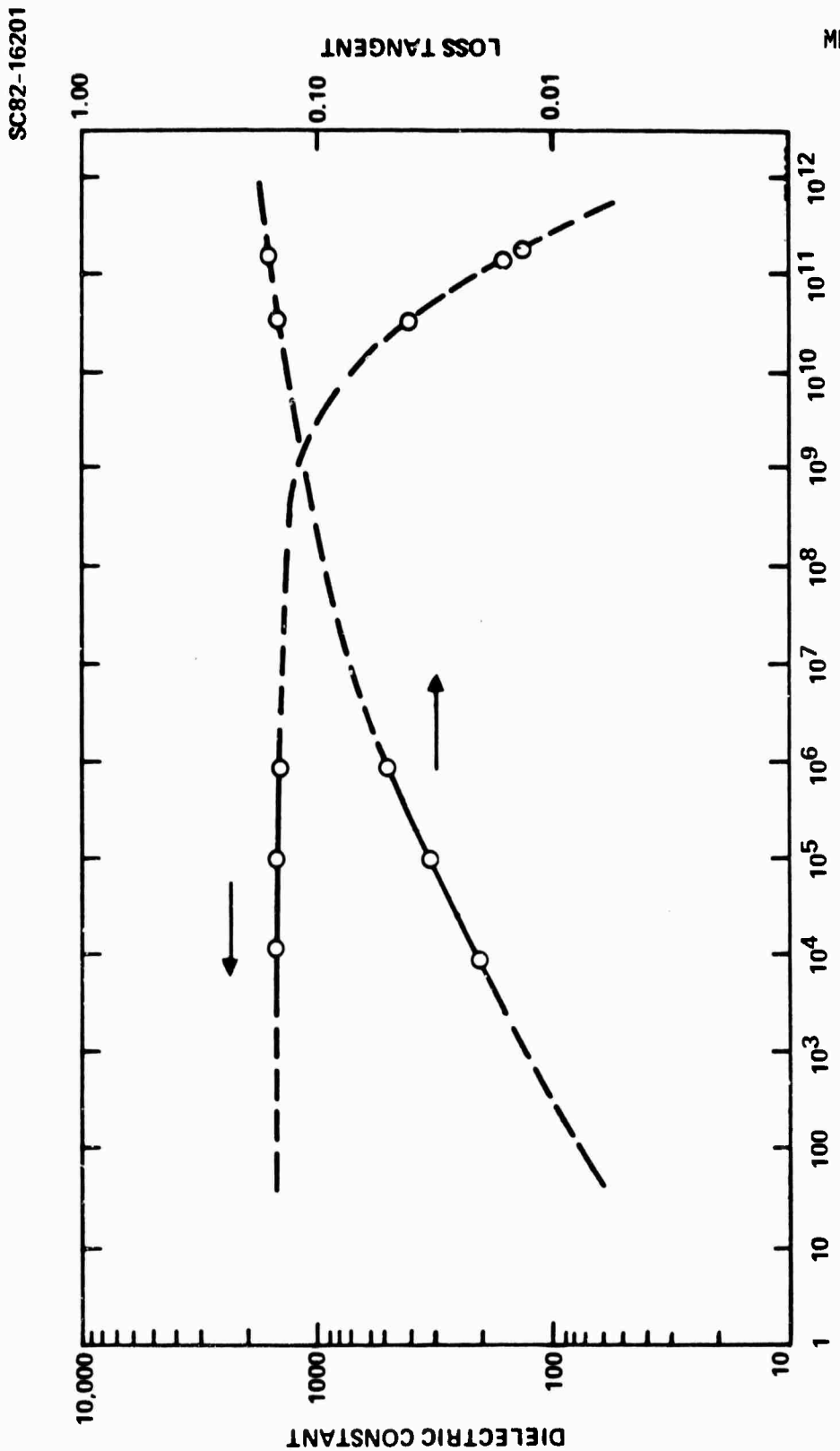

Fig. 14 Room temperature dielectric properties of ceramic PLZT (La = 10%, Zr/Ti = 80/20).

SC82-16202

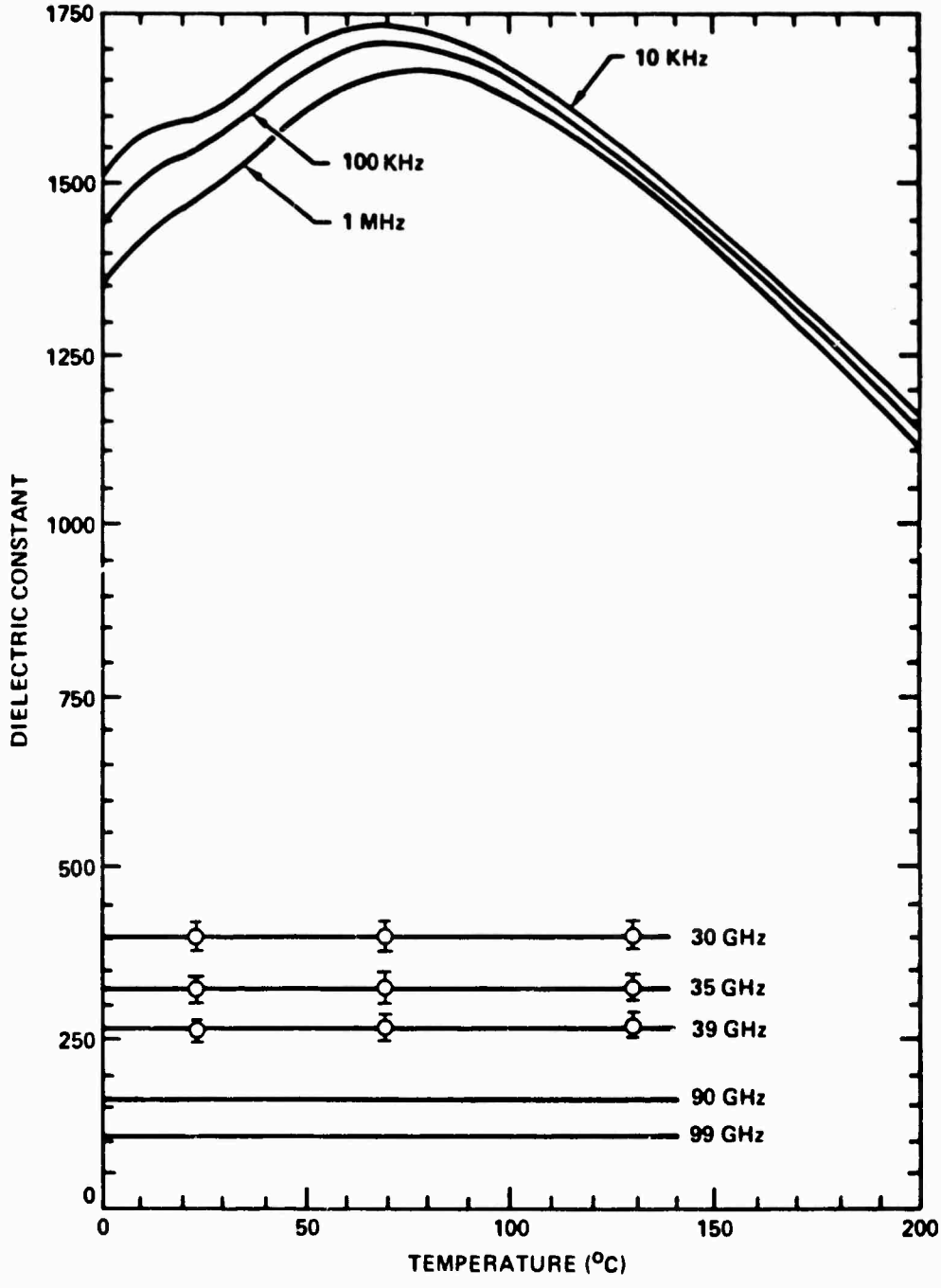

Fig. 15 Dielectric constant variation with temperature for PLZT (La = 10%, Zr/Ti = 80/20).

4.0 MATERIALS DEVELOPMENT

4.1 Materials Systems of Interest

4.1.1 Tungsten Bronze Family

Among oxide ferroelectrics, the very large family of bronze structure crystals offers a very broad range of ferroelectric properties with the possibility to "fine tune" response by composition manipulation, and consequently is of major interest. For the composition $Sr_{0.61}Ba_{0.39}Nb_2O_6$, earlier DARPA-sponsored studies have permitted the development of a full Gibbs function, and there is indication that the important higher order stiffness parameters of the prototype do not change markedly with cation make-up.

Preliminary calculations using this Gibbs function gives values of $(\partial n_3/\partial E_3)$ at 20°C

$$\partial n_3/\partial E_3 \cong -2.5 \times 10^{-6}/Vm^{-1}$$

in reasonable accord with measurements at GHz frequencies.

In the ferroelectric phase, the response increases to

$$\partial n_3/\partial E_3 \cong -6 \times 10^{-5}/Vm^{-1}$$

at 50°C, and it will be interesting to see if this trend is confirmed by measurements.

Initial calculations for the biased quadratic response suggest that the sensitivity may be vastly improved by operation in this mode. At 82°C under a bias field of 1 Kv/cm, we calculate an induced linear response

$$\partial n_3/\partial E_3 \cong -5 \times 10^{-3}/Vm^{-1} \quad ,$$

more than 3 orders larger than the room temperature response. It must be noted, however, that the response is a strong function of both temperature and bias field in this mode; however, some high frequency measurements in this regime are clearly required.

A second family of bronze structure crystals which may be of interest is the $(Na_xK_{1-x})_2(Ba_ySr_{1-y})_4Nb_{10}O_{30}$ compositions. In these crystals, all A_1 and A_2 sites in the structure are filled and there is some indication that the dielectric loss levels may be lower.

A third bronze family of interest is the $Pb_{1-x}Ba_xNb_2O_6$ compositions. In this system, increasing lead content results in the appearance of an orthorhombic ferroelectric phase with a morphotropic phase boundary near the composition $Pb_{0.6}Ba_{0.4}Nb_2O_6$. The high transverse Curie point θ for tetragonal compositions near morphotropy leads to unusually high ε_{11} and d_{15} values, and thus the possibility of large values of r^1_{11} and r^1_{15}.

4.1.2 Perovskite Family

Single crystals of perovskite structure ferroelectrics are difficult to grow and process to single domain configuration. In all materials, both pure ferroelectric and partial ferroelastic:ferroelectric domains occur due to the very high symmetry (m3m) of the prototype paraelectric phase. Since Gibbs functions are available for $BaTiO_3$, $KNbO_3$, $KNb_{1-x}Ta_xO_3$ and $PbZr_{1-x}Ti_xO_3$ systems, one can calculate the dielectric saturation functions for the singie domain states in these families. We do not, however, anticipate major advantage over the bronze structure family crystals.

The feature in the perovskite family which is, however, of major importance is the multiaxial character of the ferroelectric response, which leads to interesting and useful dielectric, piezoelectric and electro-optic response in the ceramic form. For the polar ferroelectric phases, the complex domain structures, grain to grain constraints, the highly anisotropic nature of the single domain permittivity and the difficulty of processing to a perfect single phase assemblage may make interpretation of the response diffi-

cult. In the paraelectric phase, however, many of these difficulties are eliminated, and we expect that the quadratic response will be of more interest.

A characteristic of the ceramic which may be of significant interest in developing a high quadratic response at low applied voltage is the manner in which perovskite type ceramics may be processed to produce a highly reduced conducting grain structure, separated by an insulating grain boundary region. In $BaTiO_3$-based capacitors made by this type of processing, "effective permittivities" greater than 100,000 can be achieved, indicating field multiplication by a factor of 50 or more across the grain boundary region.

Since in a quadratic system the induced response varies as E^2, the field amplification factor A augments the optical path length by a factor proportional to A^2, while the relief of field over the bulk of the grain only reduces the path length by a factor 1/A. For conducting levels ~10 ohm cm in the grain which should be adequate to provide short time constants for the application of bias field to the boundary region, the impedance of the grain at high microwave or mm wave frequencies would not be affected. In effect, the reduced grains then provide a simple method for intercalating "transparent" electrodes into the volume of the sample.

4.1.3 SbSI Family Materials

The uniaxial ferroelectric antimony sulphur iodide, together with bromide and selenide solid solutions, form another interesting family where the Gibbs function is known. Since it is difficult to raise the true Curie temperature beyond 18°C in this system, the primary interest is in the quadratic or biased quadratic mode. Initial calculations suggest that at 32.5°C, under bias of 4.5×10^3 volts/cm, the induced linear effect gives $(\partial n_3/\partial E_3)$ values of the order 10×10^{-3} Vm^{-1}.

It would appear that the materials in this family have promising prospects and more detailed evaluation is certainly in order.

5.0 FUTURE PLANS

The search for low-loss ferroelectric systems will continue as a high priority in the remainder of the contract period. Variations in loss and permittivity within SBN crystals will be related to composition and growth conditions as a first step toward uncovering the factors controlling these variations. Available systems in which other ferroelectric mechanisms are operative will also be studied.

Measurements of dn/dE will be carried out on the most interesting ferroelectrics at 35 and 94 GHz, including correlation with the observed variability in sample dielectric properties. A key question is to what extent the electric field sensitivity of the index scales with the microwave index in the SBN system.

Another important issue is the utility of variable index materials in millimeter wave radar systems. It is planned to interact with the user community to identify the current needs in terms of millimeter wave discrete and distributed active devices and to establish the materials criteria and the design of devices which can potentially meet these needs.

6.0 PUBLICATIONS AND PRESENTATIONS

6.1 Publications

1. R. R. Neurgaonkar, W. K. Cory, W. W. Ho, W. F. Hall and L. E. Cross, "Tungsten Bronze Family Crystals for Acoustical and Dielectric Applications," Ferroelectrics, 38, 857, 1981.

2. W. W. Ho, W. F. Hall, R. R. Neurgaonkar, R. E. DeWames and T. C. Lim, "Microwave Dielectric Properties of $Sr_{0.61}Ba_{0.39}Na_2O_6$ single crystals at 35 and 58 GHz," Ferroelectrics, 38, 833, 1981.

6.2 Presentations

1. R. R. Neurgaonkar, W. K. Cory, W. W. Ho, W. F. Hall and L. E. Cross, "Tungsten Bronze Family Crystals for Acoustical and Dielectric Applications," presented at the 5th International Meeting on Ferroelectricity, Penn State University, Pa., August 17-21, 1981.

2. W. W. Ho, W. F. Hall, R. R. Neurgaonkar, R. E. DeWames and T. C. Lim, "Microwave Dielectric Properties of $Sr_{0.61}Ba_{0.39}Nb_2O_6$ Single Crystals at 35 and 58 GHz," presented at the 5th International Meeting on Ferroelectricity at Penn State University, August 17-21, 1981.

7.0 REFERENCES

1. R. E. DeWames, W. W. Ho, W. F. Hall, R. R. Neurgaonkar and T. C. Lim, Bull, APS 26, 303, 1981.

2. R. R. Neurgaonkar, M. H. Kalisher, T. C. Lim, E. J. Staples and K. L. Keester, Mat. Res. Bull. 15, 1235, 1980.

3. W. W. Ho, W. F. Hall, R. R. Neurgaonkar, R. E. DeWames and T. C. Lim, Ferroelectrics 38, 833, 1981.

4. A. A. Ballman and H. Brown, J. Cryst. Growth 1, 311, 1967.

5. P. L. Lenzo, E. G. Spencer and A. A. Ballman, Appl. Phys. Lett. 11, 23, 1976.

6. A. M. Glass, J. Appl. Phys. 40, 4699, 1969.

7. R. R. Neurgaonkar, W. K. Cory, W. W. Ho, W. F. Hall and L. E. Cross, Ferroelectrics, 38, 857, 1981.

8. K. Megumi, N. Nagatsuma, Y. Kashiwada, and Y. Furuhata, J. Mat. Sci. 11, 1583, 1976.

9. O. F. Dudnik, A. K. Gromov, V. B. Kravchenko, Y. L. Kopylov and G. F. Kunznetsov, Sov. Phys. Crystograph. 15, 330, 1970.

10. P. B. Jamieson, S. C. Abrahams and J. L. Bernstein, J. Chem. Phys. 48, 5048, 1968.